Plasma Sources Sci. Technol. **5** (1996) 78–83. Printed in the UK

High current plasma electron emitter

G Fiksel†, A F Almagri†, D Craig†, M Iida‡, S C Prager† and J S Sarff†

† Department of Physics, University of Wisconsin at Madison, WI 53706, USA
‡ Kyoto Institute of Technology, Matsugasaki Sakyoky, Kyoto 606, Japan

Received 30 June 1995, in final form 12 September 1995

Abstract. A high current plasma electron emitter based on a miniature plasma source has been developed. The emitting plasma is created by a pulsed high current gas discharge. The electron emission current is 1 kA at 300 V with a pulse duration of 10 ms. The prototype injector described in this paper will be used for a 20 kA electrostatic current injection experiment in the Madison symmetric torus reversed-field pinch. The source will be replicated in order to attain this total current requirement. The source has a simple design and has proven to be very reliable in operation. A high emission current, small size (3.7 cm in diameter) and low impurity generation make the source suitable for a variety of fusion and technological applications.

1. Introduction

A variety of technological and fusion applications demand a high current, efficient electron injector. The spectrum of technological applications is very broad, including plasma sources, ion and electron beams, plasma processing, etc. Electrostatic current injection has been used in fusion plasma, usually on a small scale, for many years. For example, low current tokamak plasmas has been produced and sustained by electrostatic injection (often called dc helicity injection) [1], H-mode plasmas have been produced with biased electrodes [2], impurity generation has been controlled by biased electrodes [3], and plasma flow has been channelled by $\boldsymbol{E}\times\boldsymbol{B}$ effects induced by divertor plate biasing [4].

The plasma injector described in this paper was created for a specific task requiring current injection in the Madison symmetric torus [5] (MST) reversed field pinch (RFP) for the suppression of tearing instabilities and reduction of transport through a modification of the plasma current profile [6]. The injected current could reduce the current density gradient which drives the fluctuations which are known to produce transport [7, 8]. Nevertheless, the source appears to be very versatile with a scope of applications far beyond these specific studies.

A common source of injected current is a biased electrode, usually either metal or hot (thermo-emissive) lanthanum hexaboride. Two dominant disadvantages of these techniques are that the presence of biased material surfaces gives rise to strong plasma–electrode interactions with consequent impurity generation and reflux, and the emitted current density is limited by material thermionic emission properties. In addition, during experiments with these types of electrode in the MST we discovered that the emitted current does not exhibit the directionality required for current profile control.

We have proposed and tested a different kind of current injector that alleviates these problems. The key feature of the injector is that electrons are extracted from a miniature plasma source, rather than from an emissive material surface. The result is a source with low impurity generation, high current density and effective direction control in comparison to typical metal electrodes. In this paper we present a detailed description of a prototype 1 kA electron injector. The source is described in section 2, injector optimization studies in section 3, and an optimized current injector for MST application in section 4. This 1 kA injector will be replicated to implement a full scale 20 kA current injection system for current profile control studies in the MST.

2. The plasma source

Various types of plasma cathode have been studied [9, 10] for ion and electron beam applications. There are commercial products available that can be adjusted for various needs, for example, Spectra-Mat Inc, CA [11] manufactures electron and ion injectors based on hollow cathode plasma sources with a total electron emission current of $\sim$ 10 A. A 1 kA low energy electron-beam source based on a plasma emitter is described in [12]. For our specific requirements, among which are high per-unit emission current ($\sim$ 1 kA), small source size, and compatibility with fusion research grade plasmas, we had to design a novel plasma electron injector.

A schematic diagram of the injector is shown in figure 1. The injector contains a miniature plasma source in which a cylindrical hydrogen arc plasma is produced [13–15]. A stack of molybdenum washers 1.5–2 cm high with inner diameter 0.6–1.0 cm defines the arc channel between

0963-0252/96/010078+06$19.50

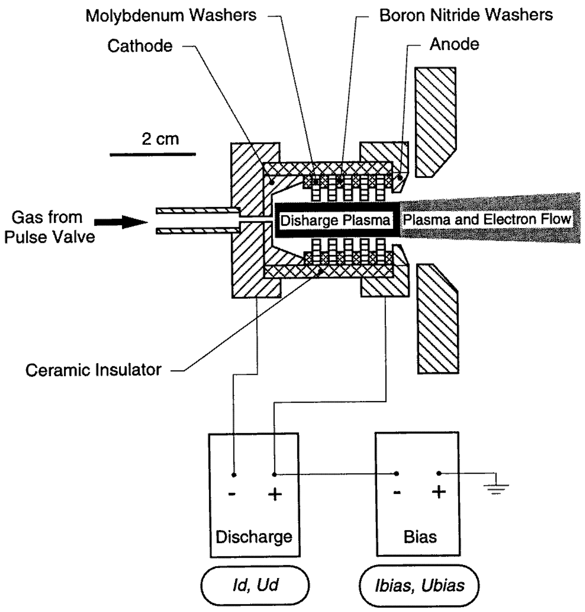

Figure 1. Schematic diagram of the plasma current injector—straight configuration.

an anode and cathode which are also made of molybdenum. The washers are isolated from each other by 1 mm thick boron nitride washers. Gas is supplied through the cathode with a pulsed electromagnetic valve, and the arc plasma is maintained by a pulse forming network. The discharge voltage is about 80–100 V, and the discharge current can be varied from 0.5 to 3 kA. The discharge duration can be varied up to 10 ms depending on the power supply. The plasma density and the temperature are controlled by the discharge current and the feeding gas flow rate. The plasma density measured at the source [14] exit is $n \approx (1\text{–}3)\times 10^{14}$ cm^{-3} and the electron temperature is $T_e \approx 10$–20 eV.

The plasma source can operate without a magnetic field, although an axial magnetic field greatly improves the source efficiency. When the source is submerged into a magnetic field the outcoming plasma is streaming along the magnetic field lines. By biasing the source with respect to another electrode (i.e. vacuum vessel wall) a flow of electrons is established relative to the plasma stream. The streaming plasma acts as a space charge neutralizing media, therefore a high electron current can be established without space charge limitation. We want to point out here that this source does not have a conventional electron beam extraction system, but rather the acceleration of electrons takes place at the near-anode plasma sheath. Nevertheless, we refer to this electron flow as a beam since it preserves its energy far from the source. (The mean collision free path for a 200 eV electron in a 10^{13} cm^{-3} background density is of the order of 10^3 cm). A similar terminology and approach is practised by authors of [12].

This plasma source design provides the user with a very high degree of flexibility in adjusting the source geometry to fulfil specific needs. The plasma chamber geometry is easy to modify, a feature which we exploited in our optimization experiments. The arrangement and the material of supporting isolators, configuration of current carrying electrodes, etc can be varied significantly while retaining the cylindrical washer–stack discharge chamber geometry and without affecting the physical properties of the plasma. An example of a different configuration of the plasma source is shown in figure 2. While being identical in the geometry of the plasma chamber, these two configurations differ in the shape of the source. We used these two configurations in different experimental set-ups. The first configuration, 'straight', utilizes the axial geometry of the magnetic field and the stand vacuum vessel. This was mainly used in our optimization experiments in the test stand. The second configuration, 'angled', is used for the current injection in the MST. The plasma source is inserted radially through a machine port and can be rotated to inject either poloidal or toroidal current. Incidentally, the straight configuration can be used in experiments for which radial injection is needed.

Table 1. List of parameters for three plasma gun configurations.

Configuration	I	II	III
Discharge channel length (cm)	3.0	3.0	1.7
Discharge channel diameter (cm)	1.0	0.6	0.6

3. Injector optimization studies

We have performed source optimization studies in order to evaluate and minimize the gas throughput and to maximize the injection current. The straight gun was used in these experiments. The variable parameters in the experiment were the discharge chamber dimensions. Three gun configurations were tested within the parameters shown in table 1.

The experimental test stand set-up with pertinent diagnostics and power supplies is shown in figure 3. The plasma source was attached to a vacuum vessel with a volume of $V_{ves} = 10^5$ cm^3. The source was immersed in a 0.1 T magnetic field created by a set of Helmholtz coils. The magnetic field was uniform in the source region and diverging farther in the vessel. The gun was isolated from the vessel with a Plexiglas flange and was biased with respect to the vessel.

The injected beam current I_{beam} was measured with a beam monitor formed by a Rogowski coil embracing the beam. The beam current density J_{beam} profile was measured by a miniature movable Rogowski coil located 60 cm from the source. The gas density in the vessel was measured by an absolutely calibrated fast ion gauge. The plasma flow generated by the source was measured with a movable ion collector. In addition, we monitored the discharge voltage U_d, discharge current I_d, bias voltage U_{bias} and bias circuit current I_{bias}.

The waveforms of the discharge current I_d and the gas throughput rate I_{gas} for a pulse duration of 2.5 ms are shown in figure 4. The gas rate in equivalent amps was

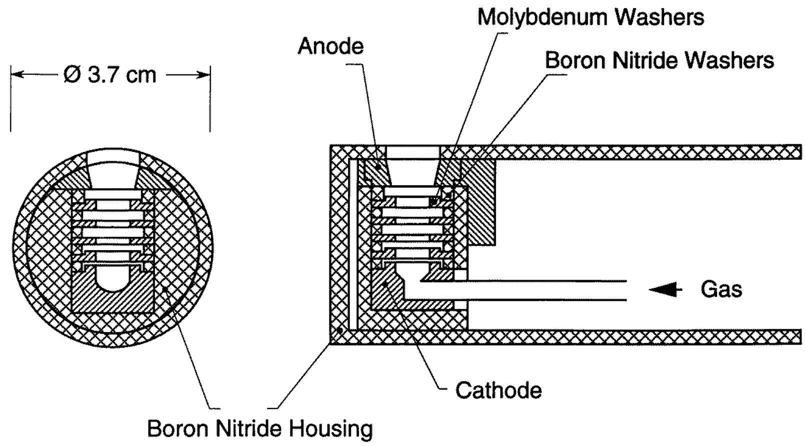

Figure 2. Schematic diagram of the plasma current injector—angled configuration. This figure also represents the MST current injector.

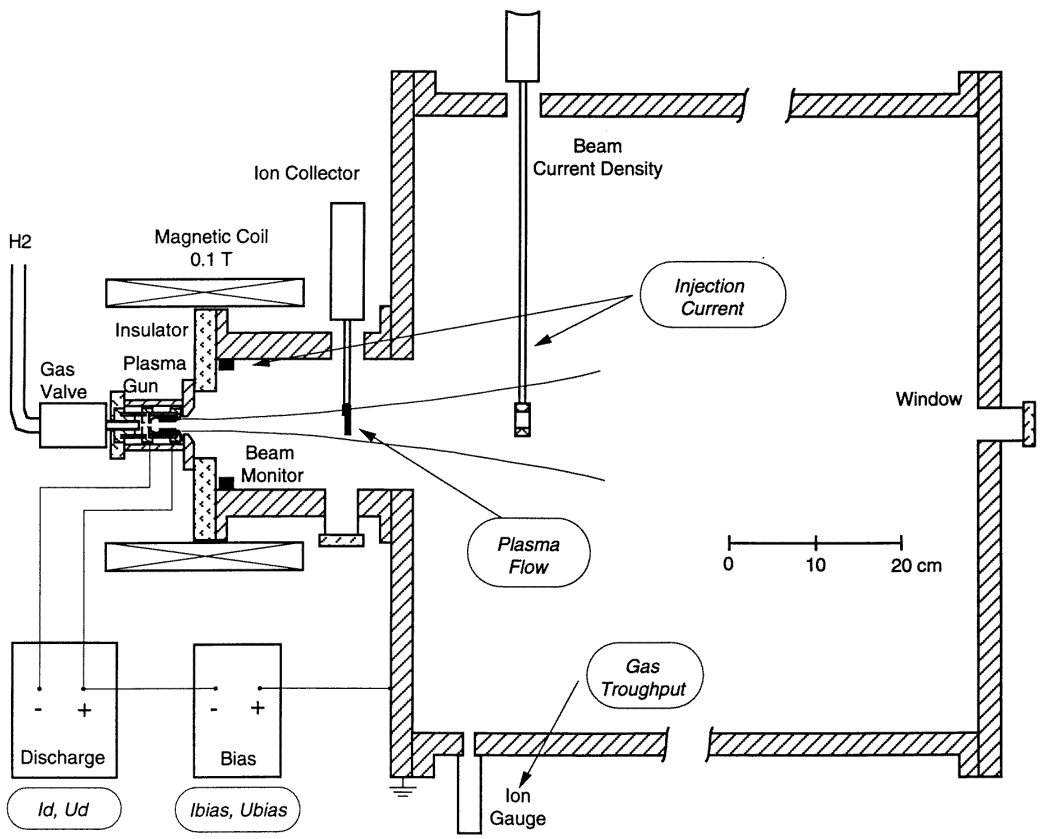

Figure 3. Test stand—experimental set-up, diagnostics and their functions.

calculated using

$$I_{gas} = 2eV_{ves}\frac{\mathrm{d}N_{H_2}}{\mathrm{d}t}$$

where N_{H_2} is the hydrogen neutral density (pressure) in the vessel measured by the fast ion gauge and e is the electron charge. We include the fact 2 in order to estimate the gas utilization when compared to the H^+ ion flow from the gun. The gas rate was adjusted by changing the gas pressure in the valve.

In order to measure the gas efficiency of the source we varied the discharge current at a given gas throughput rate and measured the ion current density J_i in the plasma flow. We also monitored the discharge voltage as an operational parameter of the discharge. We then repeated this for different throughput rates and the results for gun type I are shown in figure 5. For other configurations the results are similar.

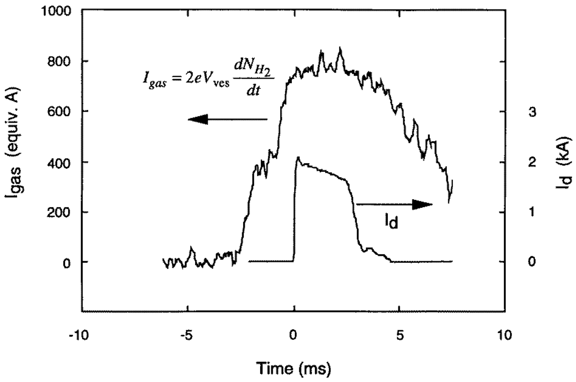

Figure 4. Waveforms of the plasma source discharge current and gas throughput rate.

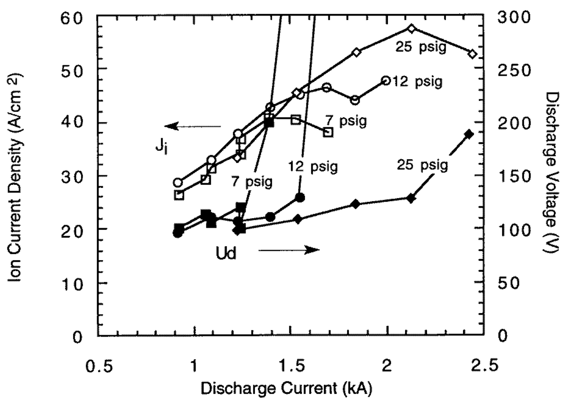

Figure 5. Measurements of gas efficiency. Plasma flow ion current density (J) and the discharge voltage (U_d) versus discharge current (I_d) at different valve pressures (throughput rates). The gas valve pressure in psig is indicated on the curves.

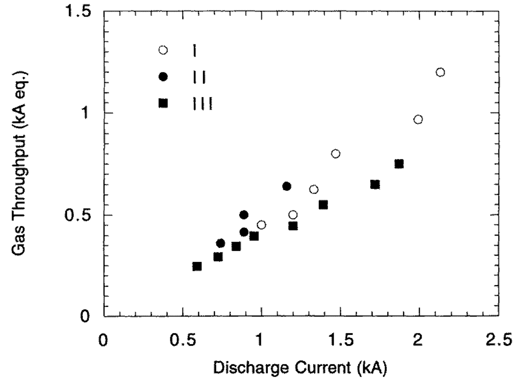

Figure 6. The minimum gas throughput rate I_{gas} versus the discharge current I_d. The gun configuration is indicated in the figure. The configuration sizes are I, 1 cm × 3 cm; II, 0.6 cm×3 cm; III, 0.6 cm×1.7 cm.

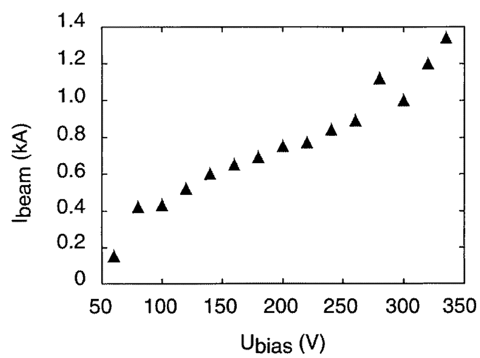

Figure 7. Injected current I_{beam} versus bias voltage U_{bias} at the discharge current I_d = 1. kA.

We see that for a given gas throughput rate there is an inflection point on the discharge voltage curve that corresponds to the maximum plasma production at a given throughput rate. Beyond that point the discharge voltage is increasing sharply over the nominal 90–100 V and plasma production remains constant or even decreases. Below the inflection point the plasma production does not depend on the gas throughput and is proportional to the discharge current. Thus, this point corresponds to a maximum in the efficiency of the plasma source. The dependence of I_{gas} on I_d measured at this point is shown in figure 6 for different gun types. Under the optimized conditions the spatially integrated ion current density profile yielding the total ion flow $I_i \approx 0.1 \times I_d$ and $I_i \approx 0.3 \times I_{gas}$. Note that during the pulse the gas outflow from the source can be significantly lower due to a high ionization ability of the plasma.

When a bias voltage is applied the injected current flows along the magnetic field lines. The current is space charge neutralized due to the outcoming plasma, so the injector can be used for injection into vacuum as well as into other plasmas. The dependence of the injected current I_{beam} on the bias voltage U_{bias} at the discharge current $I_d = 1$ kA is shown in figure 7. We have found that there are two regimes of the injection differentiated by the relative steady-state amplitudes of the discharge current I_d and the beam current I_{beam} These regimes are illustrated in figure 8 for $I_d = 1.2$ kA. When $I_{beam} \leq I_d$, the waveforms of the total beam current and beam current density are identical to each other and to that of the discharge current—figure 8(b). The spatially integrated current profile is equal to the total beam current I_{beam} and to the bias circuit current I_{bias} When $I_{beam} > I_d$, the waveform of the beam current becomes irregular (figure 8(c)) and the current profile widens. At the same time distinct arcing activity is observed on the anode surface. We identify the arcing activity by visible bright sparks on the surface and an increase in the H_α signal as monitored through a window opposite the gun. The results are similar for all gun configurations tested.

The fact that the maximum regular waveform injected current from the source is equal to the discharge current implies that in this case we divert all the discharge electrons in the source that otherwise would be collected on the anode and return them in the circuit through the injected current. When the injected current exceeds this limit, the extra electrons come through the arcing on the anode surfaces which is accompanied by broadening of the beam profile and irregular waveforms. In addition, the impurities generated by the arcing on the anode would contaminate the target plasma.

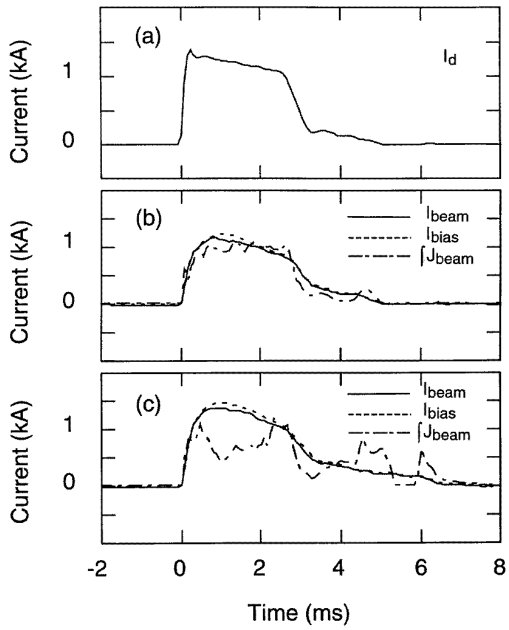

Figure 8. Waveforms of the discharge current I_d = 1.2 kA, injected current I_{beam}, bias circuit current I_{bias}, and spatially integrated beam current density $\int J_{beam}$. The figure illustrates transition from (b) $I_{beam} < I_d$ to (c) $I_{beam} > I_d$.

To summarize, we consider the optimum operational regime to be that in which the extracted current I_{beam} is equal to the discharge current I_d and the gas throughput rate is minimized according to figure 6.

4. Optimized current injector for the MST

The geometry and the size of the current injector for the MST is primarily dictated by the choice of access ports. It has been decided that the injectors will be inserted through the MST diagnostic ports which have a diameter of 3.8 cm (1.5″). Therefore, the outer diameter of the source was set at 3.7 cm and the discharge channel geometry was chosen to be that of type III. The cross-section of the injector is sown in figure 2.

The amplitude of the discharge current is limited by the duration of the plasma pulse. The current injection duration should be greater than the MST plasma energy confinement time which is several milliseconds. On the other hand, the power deposition in the gun electrodes, allowed background pressure increase, and the pumping ability put an upper bound on the pulse length. As a compromise, the current injection duration was chosen to be 10 ms. Numerical simulations and experimental data extrapolation show that for a discharge time of 10 ms a discharge current of 1 kA is appropriate from the thermal load point of view. At this discharge current and duration the total amount of required hydrogen is $\sim 10^{19}$ molecules. Recall that during the injection the actual number of injected neutrals is probably lower due to a high degree of ionization.

The injector is enclosed in a boron nitride housing with an outer diameter of 3.7 cm and inserted through a port in the MST vessel. The position of the injector is normally 4–5 cm from the wall and the bias voltage is applied with respect to the vacuum vessel. In the experiments the injector was aligned parallel to the magnetic field, which was directed poloidally near the vessel wall. The injected current profile was measured with a miniature movable Rogowski coil situated at some distance (20–70 cm) from the gun in the poloidal direction and on the magnetic field line linking the gun. This experimental set-up is illustrated in figure 9.

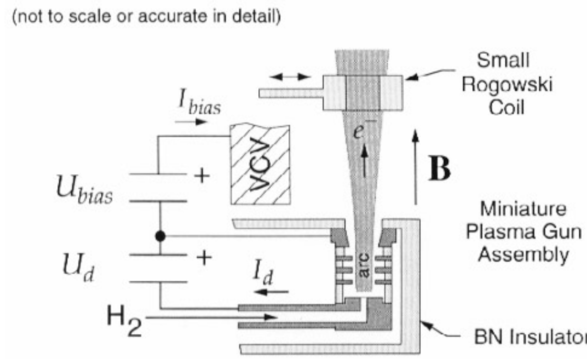

Figure 9. Schematic diagram of a typical plasma gun experiment in the MST.

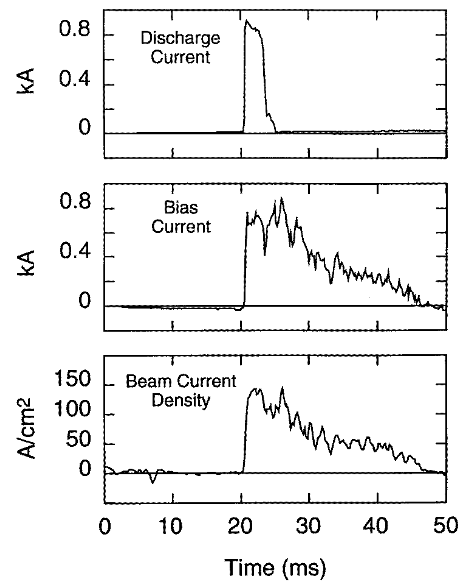

Figure 10. Current injection in MST. Waveforms of the gun discharge current I_d, injected beam current I_{beam} and beam current density J_{beam}.

The waveform of the injected current is shown in figure 10. In this example, the gun plasma is formed 20 ms after the background MST plasma is initiated, and then V_{bias} is applied at 20.5 ms. Note that a limitation in the arc power supply allow an I_d pulse of only about 3 ms, but I_{bias} can be maintained much longer. We speculate that the internal discharge initiated by the arc power supply is not completely extinguished but is rather sustained to some degree through combined action of the bias power supply and the MST plasma. In general, the gun operates optimally

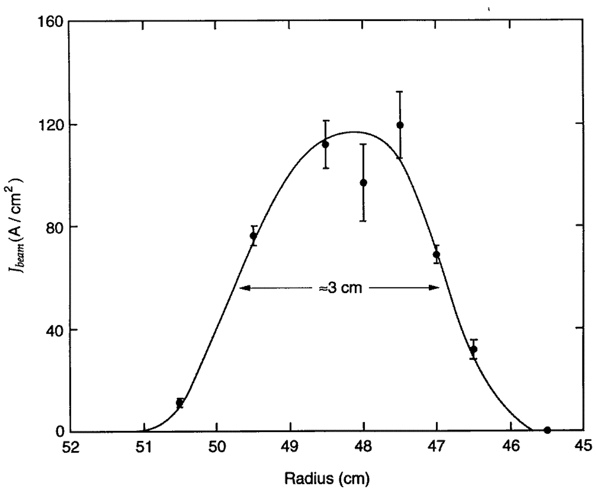

Figure 11. Radial profile of the emission current measured with a movable Rogowski coil. The gun is located on the flux surface at 48 cm, separated from the Rogowski by 25 cm (poloidal angular separation of 30°). 52 cm corresponds to the vessel wall. The plasma center is located at 0 cm. The total emission current is 1 kA, the arc current is 1 kA, and the emission bias voltage is 270 V.

when $I_d = I_{bias}$ which agrees with the optimization studied on the test stand. Without first establishing the arc plasma, emission is irregular and not reproducible. Therefore, we plan to use a 10 ms arc power supply with a 10 ms bias power supply in our future injection experiments.

The injected current profile at a discharge current of 1 kA and a bias voltage of 270 V is shown in figure 11. The measured maximum emission current density is high (e.g. 100 A cm^{-2}–120 A cm^{-2} at the peak) and the radial extent is about 3 cm. The profile integrated total current was about 1 kA which is about equal to the bias circuit current. This fact implies that the injected current has a high degree of directionality. The high directionality was also confirmed by rotating the gun through 180°. Virtually all of the current emitted from the gun is observed in the forward direction as required for efficient current profile modification.

The impurity generation was measured with the MST diagnostics which included monitoring of line intensities of impurities (C, O, Al) as well as the total radiated power. Previously tested metal electrode injectors generated a significant influx of impurities which sometimes terminated the MST plasma. We did not detect a change in the impurity level while operating the plasma injector. It appears that this is due to the high plasma density and temperature in the source the impurities are ionized and remain trapped in the plasma column. We are currently installing a VUV spectrometer for the diagnostics of Mo lines.

5. Conclusions

We have developed a plasma electron injector for fusion and technological applications. The injector is based on a miniature plasma source and utilizes its plasma as an electron emitter. The nominal parameters of the injector are: size—3.7 cm in diameter and 6 cm (not critical) in length, emission current—1 kA, emission voltage—250–300 V, pulse duration—10 ms, gas requirements—10^{19} molecules/pulse.

The prototype source described in this paper will be replicated for the MST injection in order to attain this total current requirement of 20 kA. Each gun will have its own arc and emission power supplies providing a 10 ms injection pulse. The scope of technological application of the injector includes electron emitters, ion and electron beams, and plasma processing.

Acknowledgments

The authors are grateful for the assistance of C-S Chiang, R Kendrick, T W Lovell, S Oliva and M Thomas. This work was supported by the US Department of Energy.

References

[1] Forest C B, Hwang Y S, Cho M and Darrow D S 1992 *Phys. Rev. Lett.* **68** 3559
[2] Taylor R J, Brown M L, Fried B D, Grote H, Liberati J L, Morales G J and Pribyl P 1989 *Phys. Rev. Lett.* **63** 2365
[3] Taylor R J and Oren L 1979 *Phys. Rev. Lett.* **42** 446
[4] Schaffer M J, Ali Madhavi M, Kepler C C, Hill D N and Rensing M E 1991 *Bull. Am. Phys. Soc.* **36** 2325
Strait E J 1981 *Nucl. Fusion* **21** 943
[5] Dexter R N, Kerst D W, Lovell T W, Prager S C and Sprott J C 1991 *Fusion Technol.* **19** 131
[6] Sarff J S *et al* 1995 *Phys. Plasmas* **2** 2440
[7] Fiksel G, Prager S C, Shen W and Stoneking M R 1994 *Phys. Rev. Lett.* **72** 1028
[8] Stoneking M R, Hokin S A, Prager S C, Fiksel G, Ji H and Den Hartog D 1994 *Phys. Rev. Lett.* **73** 549
[9] McGeogh M 1991 *J. Appl. Phys.* **71** 1163
[10] Shibuya T, Hashimoto S, Yabe E and Takayama K 1991 *Nucl. Instrum. Methods* B **55** 305
[11] *Catalog* Spectra-Mat, Inc., 100 Westgate Dr., Watsonville, CA 90576, USA
[12] Hamagaki M, Hara T, Sadamoto Y and Ohgo T 1995 *Rev. Sci. Instrum.* **66** 3469
[13] Dimov G I and Roslyakov G V 1974 *Sov. Prib. Tech. Exp.* **1** 29
[14] Fiksel G 1991 *PhD Thesis* University of Wisconsin-Madison
[15] Fiksel G, Hershkowitz N and Kishinevsky M 1991 *Phys. Fluids* B **3** 834